

# **IMPROVING LESION SEGMENTATION FOR BREAST CANCER DETECTION**

## **Submitted By**

Md. Monjurul Islam (112441)  
Mobasshir Hossain Akash (112443)  
Shah Md. Injamamul Islam (112457)

## **Supervised By**

Md. Taslim Reza  
Assistant Professor,  
Department of Electrical and Electronic Engineering,  
Islamic University of Technology (IUT), Bangladesh.

# **IMPROVING LESION SEGMENTATION FOR BREAST CANCER DETECTION**

**Approved By**

---

Md. Taslim Reza  
Assistant Professor,  
Department of Electrical and Electronic Engineering,  
Islamic University of Technology (IUT), Bangladesh.

## **Project Members**

1. Md. Monjurul Islam  
Student Id: 112441

---

2. Mobasshir Hossain Akash  
Student Id: 112443

---

3. Shah Md. Injamamul Islam  
Student Id: 112457

---

# Abstract

Breast cancer is the most common cause of death among patients and one of the main reasons is that the lesion is not identified properly. Ultrasound images are very difficult to segment due to presence of speckle noise and the boundaries of abnormal regions are too difficult to recognize due to similarity. For this reason, proper medical facility or treatment cannot be provided in time. The situation in Bangladesh is alarming as there is a huge female population in the rural areas who don't have proper medical access to detect the early stage of breast cancer.

We have implemented a Computer Aided Diagnosis (CAD) system that will detect the cancerous lesion in the BUS (breast ultrasound) images effectively. We implemented a region growing algorithm which can segment the object of interests (lesion). We place the seed on the ultrasound image (original image), check homogeneity and merge the homogeneous regions. After that we use horizontal cut based entropy filtering and at last by canny edge detection we subtract the object of interests (lesion) from the desired ultrasound image. We also implemented developed watershed algorithm and assimilated it with region growing algorithm.

Keywords: Entropy, SRAD Filtering, Watershed Segmentation, Binary Thresholding, Canny Edge Detection.

# Acknowledgements

First and foremost, we offer gratitude to the Almighty Allah (SWT) for giving us the capability to do this work with good health.

We are grateful to our research supervisor, Md. Taslim Reza, for the support and guidance throughout our research at Islamic University of Technology (IUT) since September, 2014. He created a research environment for which we were able to explore many ideas without constraint. We have gained a wealth of knowledge and experience in science and engineering through his direction that is beyond value to our future endeavor. For this things we give many things to him.

We are very grateful to Dr. S. Kaisar Alam, Visiting Professor, CBIM, Rutgers University, New Jersey, U.S.A. for providing us with Image Database. And we are also very thankful to Rashid-Al-Mukaddim, Lecturer, Department of EEE, IUT foe extending help towards us whenever we were in need of it.

We would like to thank all the faculty members of the department of EEE, IUT for their inspiration and help.

And last but not the least we are thankful to our family, friends and well-wishers for their support and inspiration.

# Dedication

Every challenging work needs self-efforts as well as guidance of elders especially those who were very close to our heart.

Our humble effort we dedicate to our sweet and loving

Father & Mother,

Whose affection love, encouragement and prays of day and night make me able to get such success and honor,

Along with all hard working and respected

Teachers

# Table of Contents

<b>CHAPTER 1: INTRODUCTION .....</b>	<b>11</b>
1.1 BASIC .....	11
1.1 PRESENT SCENARIO.....	12
1.2 IMAGING TESTS.....	14
1.3 THESIS OBJECTIVE .....	17
<b>CHAPTER 2: ULTRASOUND IMAGING .....</b>	<b>18</b>
2.1 INTRODUCTION.....	18
2.2 BASIC PRINCIPLES OF B-MODE US .....	19
2.3 GENERATION OF ULTRASOUND PULSES .....	20
2.3 ULTRASOUND WAVELENGTH AND FREQUENCY.....	23
2.4 ULTRASOUND–TISSUE INTERACTION.....	26
<b>CHAPTER 3: CURRENT STATE OF ART .....</b>	<b>30</b>
3.1 INTRODUCTION.....	30
3.2 SEGMENTATION.....	30
<b>CHAPTER 4: SEGMENTATION METHODS .....</b>	<b>35</b>
4.1 INTRODUCTION.....	35
4.2 EXPLANATION OF DIFFERENT KINDS OF SEGMENTATION.....	35

4.2.1 WATERSHED SEGMENTATION .....	35
4.2.2 REGION BASED SEGMENTATION .....	36
4.2.3 HISTOGRAM THRESHOLDING .....	36
4.2.4 MODEL-BASED (ACTIVE CONTOUR, MARKER RANDOM FIELD) .....	37
4.2.5 MACHINE LEARNING .....	37
4.2.6 SEGMENTATION BASED ON CLUSTERING (HARD, K-MEANS, FUZZY CLUSTERING) .....	38

## **CHAPTER 5: WATERSHED SEGMENTATION.....40**

5.1 INTRODUCTION.....	40
5.2 BASIC ALGORITHM .....	41
5.3 IMPLEMENTATION .....	41
5.3.1 THE DISTANCE TRANSFORM .....	42
5.3.2 GRADIENTS .....	43
5.3.3 MARKER-CONTROLLED .....	43

## **CHAPTER 6: REGION GROWING SEGMENTATION .....51**

6.1 INTRODUCTION.....	51
-----------------------	----

## **CHAPTER 07: CONCLUSION .....62**

REFERENCE .....	63
-----------------	----



# List of figures

FIGURE 1.1: AVERAGE NUMBER OF DEATH PER YEAR AND AGE-SPECIFIC INCIDENCE RATES PER 100,000 POPULATION, FEMALES, UK (CANCER RESEARCH UK) [59].....	13
FIGURE 2.1: PICTURE OF A TRANSDUCER (PROBE) USED DURING AN ULTRASOUND EXAM [62].....	20
FIGURE 2.2: GENERATING WAVE [63] .....	21
FIGURE 2.3: PIEZO ELECTRIC CRYSTAL [63] .....	21
FIGURE 2.4: WORKING METHOD OF ULTRASOUND EXAMINATION (PART-1) [63] .....	22
FIGURE 2.5: WORKING METHOD OF ULTRASOUND EXAMINATION (PART-2) [63] .....	22
FIGURE 2.6: ATTENUATION OF ULTRASOUND WAVES AND ITS RELATIONSHIP TO WAVE FREQUENCY. NOTE THAT HIGHER FREQUENCY WAVES ARE MORE HIGHLY ATTENUATED THAN LOWER FREQUENCY WAVES FOR A GIVEN DISTANCE. REPRODUCED WITH PERMISSION FROM REF. [64] .....	23
FIGURE 2.7: A COMPARISON OF THE RESOLUTION AND PENETRATION OF DIFFERENT ULTRASOUND TRANSDUCER FREQUENCIES. THIS FIGURE WAS PUBLISHED IN REF. [64] COPYRIGHT ELSEVIER (2000).....	24
FIGURE 2.8: SCHEMATIC REPRESENTATION OF ULTRASOUND PULSE GENERATION. REPRODUCED WITH PERMISSION FROM REF [64].....	24
FIGURE 2.9: ULTRASOUND WAVELENGTH AND FREQUENCY [63].....	25
TABLE 2.1: ACOUSTIC IMPEDANCES OF DIFFERENT BODY TISSUES AND ORGANS .....	26
FIGURE 2.10: DIFFERENT TYPES OF ULTRASOUND WAVE–TISSUE INTERACTIONS. REPRODUCED WITH PERMISSION [64] FROM REF.6.....	26
FIGURE 2.11: REFRACTION ARTIFACT. DIAGRAM (A) SHOWS HOW SOUND BEAM REFRACTION RESULTS IN DUPLICATION ARTIFACT. (B) IS A TRANSVERSE MIDLINE VIEW OF THE UPPER ABDOMEN SHOWING DUPLICATION OF THE AORTA (A) SECONDARY TO RECTUS MUSCLE REFRACTION. THIS FIGURE WAS PUBLISHED IN REF. [65] COPYRIGHT ELSEVIER (2004).....	28
FIGURE 2.12: DEGREES OF ATTENUATION OF ULTRASOUND BEAMS AS A FUNCTION OF THE WAVE FREQUENCY IN DIFFERENT BODY TISSUES. REPRODUCED WITH PERMISSION FROM REF. [64]..	28
FIGURE 5.1: TOPOGRAPHIC RELIEF IMAGE [60] .....	40
FIGURE 5.4: LRGB SUPERIMPOSED TRANSPARENTLY ON ORIGINAL IMAGE [61].....	45
FIGURE 5.3: COLORED WATERSHED LABEL MATRIX (LRGB) [61] .....	45
FIGURE 5.2: ORIGINAL IMAGE [61] .....	45
FIGURE 5.5: ULTRASOUND IMAGE (ORIGINAL IMAGE) .....	46
FIGURE 5.6: WATERSHED RGB IMAGE .....	46

FIGURE 5.7: BINARY THRESHOLDING IMAGE.....	47
FIGURE 5.8: 3×3 IMAGE NEIGHBORHOOD.....	48
FIGURE 5.9: AFTER SOBEL EDGE DETECTION .....	49
FIGURE 5.10: SEGMENTED IMAGE (SUPERIMPOSED INTO ORIGINAL IMAGE).....	49
FIGURE 5.11: SEGMENTED IMAGE (TYPE 1).....	50
FIGURE 5.12: SEGMENTED IMAGE (TYPE 2).....	50
FIGURE 5.13: SEGMENTED IMAGE (TYPE 3).....	50
FIGURE 6.1: FLOWCHART OF REGION GROWING ALGORITHM.....	52
FIGURE 6.2: BUS IMAGE.....	53
FIGURE 6.3: SEED SELECTION.....	53
FIGURE 6.4: APPLYING REGION GROWING ALGORITHM .....	54
FIGURE 6.5: SEGMENTED IMAGE .....	54
FIGURE 6.6: ORIGINAL BUS IMAGE SHOWING ECHOGENICITY.....	56
FIGURE 6.7: SEGMENTED IMAGE (HORIZONTAL CUT BASED ENTROPY FILTERING .....	57
FIGURE 6.8: BINARY SEGMENTED IMAGE.....	57
FIGURE 6.9: DELETING BOUNDARY & CORNER CONNECTED REGIONS .....	58
FIGURE 6.10: RANKING THE BINARY IMAGE.....	58
FIGURE 6.11: APPLIED CANNY EDGE DETECTION .....	60
FIGURE 6.12: EDGE DETECTION IMAGE SUPERIMPOSED INTO BUS IMAGE .....	60
FIGURE 6.14: OUR SEGMENTED IMAGE (TYPE-2) .....	61
FIGURE 6.13: OUR SEGMENTED IMAGE (TYPE-1) .....	61
FIGURE 6.15: OUR SEGMENTED IMAGE (TYPE-3) .....	61
FIGURE 6.16: OUR SEGMENTED IMAGE (TYPE-4) .....	61

# Chapter 1

## Introduction

### 1.1 Basic

Cancer is the name given to a collection of related diseases. In all types of cancer, some of the body's cells begin to divide without stopping and spread into surrounding tissues.

Cancer can start almost anywhere in the human body, which is made up of trillions of cells. Normally, human cells grow and divide to form new cells as the body needs them. When cells grow old or become damaged, they die, and new cells take their place.

When cancer develops, however, this orderly process breaks down. As cells become more and more abnormal, old or damaged cells survive when they should die, and new cells form when they are not needed. These extra cells can divide without stopping and may form growths called tumors.

Many cancers form solid tumors, which are masses of tissue. Cancers of the blood, such as leukemia's, generally do not form solid tumors. Cancerous tumors are malignant, which means they can spread into, or invade, nearby tissues. In addition, as these tumors grow, some cancer cells can break off and travel to distant places in the body through the blood or the lymph system and form new tumors far from the original tumor. Unlike malignant tumors, benign tumors do not spread into, or invade, nearby tissues. Benign tumors can sometimes be quite large, however. When removed, they usually don't grow back, whereas malignant tumors sometimes do.

Breast cancer is a malignant cell growth in the breast. If left untreated, the cancer spreads to other areas of the body. Excluding skin cancer, breast cancer is the most common type of cancer in women in the present world, accounting for one of every three cancer diagnoses.

Breast cancer begins in the breast tissue that is made up of glands for milk production, called lobules, and the ducts that connect the lobules to the nipple. The remainder of the breast is made up of fatty, connective, and lymphatic tissues. Breast cancer typically produces no symptoms when the tumor is small and most easily cured. Therefore, it is very important for women to follow recommended screening guidelines for detecting breast cancer at an early stage. When breast cancer has grown to a size that can be felt, the most common physical sign is a painless lump. Sometimes breast cancer can spread to underarm lymph nodes and cause a lump or swelling, even before the original breast tumor is large enough to be felt.

## 1.1 Present scenario

One in eight deaths worldwide is due to cancer [1]. Cancer is the second leading cause of death in developed countries and the third leading cause of death in developing countries. In 2009, about 562,340 Americans died of cancer, more than 1,500 people a day. Approximately 1,479,350 new cancer cases were diagnosed in 2009. In the United States, cancer is the second most common cause of death, and accounts for nearly 1 of every 4 deaths [2]. Breast cancer is the most common, life-threatening cancer among American women [3]. Although breast cancer has very high incidence and death rate, the cause of breast cancer is still unknown [4]. No effective way to prevent the occurrence of breast cancer exists. Therefore, early detection is the first crucial step towards treating breast cancer. It plays a key role in breast cancer diagnosis and treatment. The technological boom in every aspect has made researchers to ponder over a screening tool that can be used to detect tumor in its developing stage, which can be used by the surgeons for further diagnosis.

There were an estimated 14.1 million cancer cases around the world in 2012, of these 7.4 million cases were in men and 6.7 million in women. This number is expected to increase to 24 million by 2035. cause of death, and accounts for nearly 1 of every 4 deaths [5]. Breast cancer is the most common, life-threatening cancer among American women [6].

This growing cancer burden, within the overall context of non-communicable diseases (NCDs), was a key focus of the September 2011 UN High Level Meeting on NCDs.

Breast cancer was the most common cancer worldwide in women contributing more than 25% of the total number of new cases diagnosed in 2012. [7]

The top three, breast, colorectal and lung cancers, contributed more than 43% of all cancers (excluding non-melanoma skin cancer). [7]

Cervical cancer also contributed nearly 8% of all cancers (excluding non-melanoma skin cancer).[7]

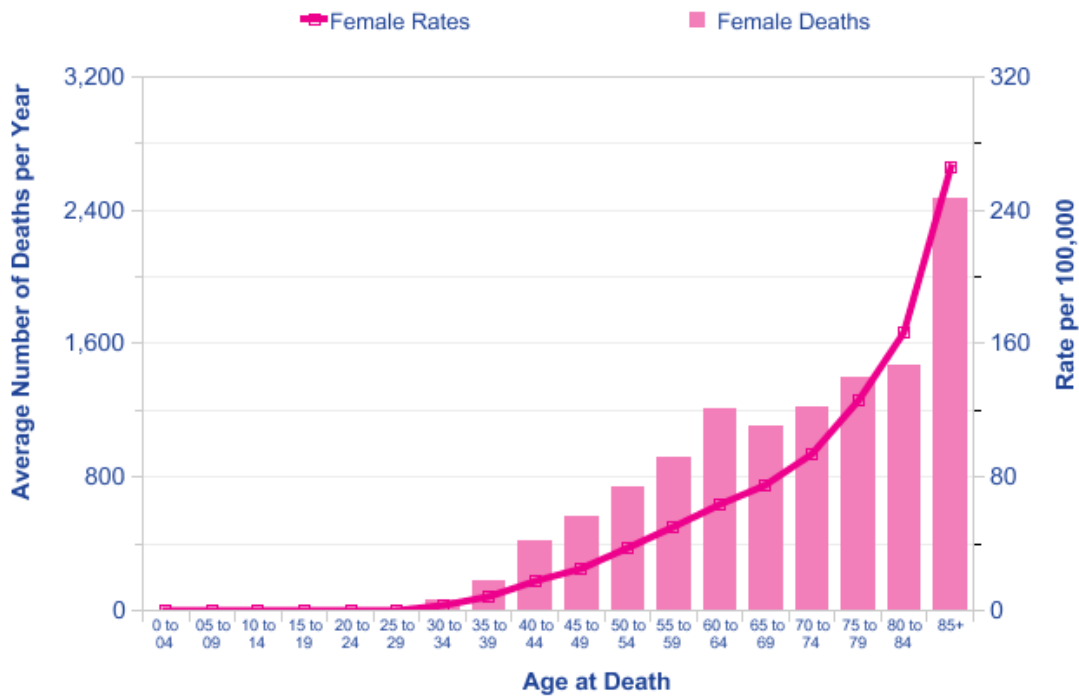


Figure 1.1: Average Number of death per year and Age-Specific Incidence Rates per 100,000 Population, Females, UK (Cancer Research UK) [59]

## 1.2 Imaging Tests

Breast cancer screening is vital to detecting breast cancer. The most common screening methods are mammography and sonography. Ultrasound imaging has proved to be a valuable addition to mammography in the detection and classification of breast lesions [8]. Due to low specificity Mammography can detect false positives resulting in unnecessary biopsy operations. Also Mammography is ineffective in detecting breast cancer in adolescent women because of ongoing breast tissue formation in that age period.

Imaging tests use x-rays, magnetic fields, sound waves, or radioactive substances to create pictures of the inside of your body. Imaging tests may be done for a number of reasons, including to help find out whether a suspicious area might be cancerous, to learn how far cancer may have spread, and to help determine if treatment is working.

### Mammograms

A mammogram is an x-ray of the breast [9]. Screening mammograms are used to look for breast disease in women who have no signs or symptoms of a breast problem. Screening mammograms usually take 2 views (x-ray pictures taken from different angles) of each breast.

For a mammogram, the breast is pressed between 2 plates to flatten and spread the tissue. This may be uncomfortable for a moment, but it is necessary to produce a good, readable mammogram. The compression only lasts a few seconds. If you have breast symptoms (like a lump or nipple discharge) or an abnormal result on a screening mammogram, you will have a diagnostic mammogram. This will include more images of the area of concern. If your diagnostic mammogram shows that the abnormal area is more suspicious for cancer, a biopsy will be being needed to tell if it is cancer.

Even if the mammograms show no tumor, if you or your doctor can feel a lump, a biopsy is usually needed to make sure it isn't cancer. One exception would be if an

ultrasound exam finds that the lump is a simple cyst (a fluid-filled sac), which is very unlikely to be cancerous.

If cancer is found, a diagnostic mammogram is often done to get more thorough views of both breasts. This is to check for any other abnormal areas that could be cancer as well.

## **Breast Ultrasound**

Ultrasound, also known as sonography, uses sound waves to outline a part of the body [9]. For this test, a small, microphone-like instrument called a transducer is placed on the skin (which is often first lubricated with ultrasound gel). It emits sound waves and picks up the echoes as they bounce off body tissues. The echoes are converted by a computer into a black and white image that is displayed on a computer screen. This test is painless and does not expose you to radiation.

Ultrasound has become a valuable tool to use along with mammography because it is widely available and less expensive than other options, such as MRI. Usually, breast ultrasound is used to target a specific area of concern found on the mammogram. Ultrasound helps distinguish between cysts (fluid-filled sacs) and solid masses and sometimes can help tell the difference between benign and cancerous tumors. In someone with a breast tumor, it can also be used to look for enlarged lymph nodes under the arm.

The use of ultrasound instead of mammograms for breast cancer screening is not recommended. However, clinical trials are now looking at the benefits and risks of adding breast ultrasound to screening mammograms in women with dense breasts and a higher risk of breast cancer.

## **Magnetic Resonance Imaging (MRI) of the breast**

MRI scans use radio waves and strong magnets instead of x-rays [9]. The energy from the radio waves is absorbed and then released in a pattern formed by the type of body tissue and by certain diseases. A computer translates the pattern into a very

detailed image. For breast MRI to look for cancer, a contrast liquid called gadolinium is injected into a vein before or during the scan to show details better.

MRI scans can take a long time – often up to an hour. For a breast MRI, you have to lie inside a narrow tube, face down on a platform specially designed for the procedure. The platform has openings for each breast that allow them to be imaged without compression. The platform contains the sensors needed to capture the MRI image. It is important to remain very still throughout the exam.

MRI can be used along with mammograms for screening women who have a high risk of developing breast cancer, or it can be used to better examine suspicious areas found by a mammogram. MRI is also sometimes used for women who have been diagnosed with breast cancer to better determine the actual size of the cancer and to look for any other cancers in the breast. It is not yet clear how helpful this is in planning surgery in someone known to have breast cancer. In someone known to have breast cancer, it is sometimes used to look at the opposite breast, to be sure that it does not contain any tumors.

If an abnormal area in the breast is found, it can often be biopsied using an MRI for guidance. This is discussed in more detail in the "Biopsy" section.

## **Biopsy**

A biopsy is done when mammograms, other imaging tests, or the physical exam finds a breast change (or abnormality) that is possibly cancer [10]. A biopsy is the only way to tell if cancer is really present.

During a biopsy, a sample of the suspicious area is removed to be looked at under a microscope, by a specialized doctor with many years of training called a pathologist. The pathologist sends your doctor a report that gives a diagnosis for each sample taken. Information in this report will be used to help manage your care.

There are several types of biopsies, such as fine needle aspiration biopsy, core (large needle) biopsy, and surgical biopsy. Each has its pros and cons. The choice of which to use depends on your specific situation. Some of the factors your doctor will consider include how suspicious the lesion appears, how large it is, where in the breast it is located, how many lesions are present, other medical problems you might



have, and your personal preferences. You might want to discuss the pros and cons of different biopsy types with your doctor.

Often, after the tissue sample is removed, the doctor will place a tiny metal clip or marker inside the breast at the biopsy site. The clip cannot be felt and should not cause any problems, but it is helpful in finding the area again on future mammograms and for surgery. Some patients who have cancer are given chemotherapy or other treatments before surgery that can shrink the tumor so much that it can't be felt or seen on mammogram. The clip can be used to direct the surgeon to the area where the tumor was so the correct area of the breast can be removed.

## **1.3 Thesis Objective**

The main objective of the thesis is to focus on devising an automatic computer aided system by combining region growing and watershed algorithms which will be capable of processing input ultrasound image accurately and precisely. For this, successful implementation of region growing (both manual and automated) and watershed algorithms is mandatory. We use the manually outlined lesions by an experienced radiologist as the golden standard and evaluated the performance by both area error metrics and boundary error metrics. Therefore, our goal is to devise a reliable, efficient and cost-effective segmentation method for early detection of Breast Cancer.

# Chapter 2

## Ultrasound Imaging

### 2.1 Introduction

Ultrasound imaging (sonography) uses high-frequency sound waves to view inside the body. Because ultrasound images are captured in real-time, they can also show movement of the body's internal organs as well as blood flowing through the blood vessels. Unlike X-ray imaging, there is no ionizing radiation exposure associated with ultrasound imaging.

The ultrasound image is produced based on the reflection of the waves off of the body structures. The strength (amplitude) of the sound signal and the time it takes for the wave to travel through the body provide the information necessary to produce an image.

Ultrasound is used in the clinical applications extensively these days. It is noninvasive, portable and more over the cost of clinical treatments with ultrasound technology is less expensive and affordable. It is not only possible to visualize the anatomy or morphology with ultrasound imaging but can also measure or predict the almost all kind of function by means of blood. Nowadays it is extensively used in fetal imaging, carding imaging, breast cancer detection, and detection of benign and malignant tissue in the human body.

Though the ultrasound frequency range starts from 20 kHz, in clinical applications we use typically a range from 1MHz to 15MHz. The typical velocity of ultrasound in the human tissue is 1540 m/s.

Today, ultrasound (US) is one of the most widely used imaging technologies in medicine. It is portable, free of radiation risk, and relatively inexpensive when compared with other imaging modalities, such as magnetic resonance and computed tomography. Furthermore, US images are tomographic, i.e., offering a “cross-sectional” view of anatomical structures. The images can be acquired in “real time,”

thus providing instantaneous visual guidance for many interventional procedures including those for regional anesthesia and pain management.

## 2.2 Basic Principles of B-Mode US

Modern medical US is performed primarily using a pulse-echo approach with a brightness-mode (B-mode) display. The basic principles of B-mode imaging are much the same today as they were several decades ago. This involves transmitting small pulses of ultrasound echo from a transducer into the body. As the ultrasound waves penetrate body tissues of different acoustic impedances along the path of transmission, some are reflected back to the transducer (echo signals) and some continue to penetrate deeper. The echo signals returned from many sequential coplanar pulses are processed and combined to generate an image. Thus, an ultrasound transducer works both as a speaker (generating sound waves) and a microphone (receiving sound waves). The ultrasound pulse is in fact quite short, but since it traverses in a straight path, it is often referred to as an ultrasound beam. The direction of ultrasound propagation along the beam line is called the axial direction, and the direction in the image plane perpendicular to axial is called the lateral direction. [66] Usually only a small fraction of the ultrasound pulse returns as a reflected echo after reaching a body tissue interface, while the remainder of the pulse continues along the beam line to greater tissue depths.



Figure 2.1: B-Mode Image of Liver [67]

## 2.3 Generation of Ultrasound Pulses

The ultrasound is generated by a piezoelectric crystal. This piezoelectric crystal is embedded in the transducer which acts both as transmitter and receiver in the ultrasound imaging process. The crystal deforms under the influence of an electric field and vice versa.

In an ultrasound exam, a transducer (probe) is placed directly on the skin or inside a body opening. A thin layer of gel is applied to the skin so that the ultrasound waves are transmitted from the transducer through the gel into the body.



Figure 2.2: Picture of a transducer (probe) used during an ultrasound exam [62]

Ultrasound imaging is based on the same principles involved in the sonar used by bats, ships and fishermen. When a sound wave strikes an object, it bounces back, or echoes. By measuring these echo waves, it is possible to determine how far away the object is as well as the object's size, shape and consistency (whether the object is solid or filled with fluid).

In medicine, ultrasound is used to detect changes in appearance, size or contour of organs, tissues, and vessels or detect abnormal masses, such as tumors.

To use ultrasound to find things, we first need to have a way of generating them. We need something to create vibrations that will travel in the tissues in a patient.



Figure 2.3: Generating Wave [63]

There is a special material called a “piezo electric crystal”. This material has a very special property. When a voltage is applied to a piezo electric crystal (shown in red below), it expands. When the voltage is removed, it contracts back into its original thickness.

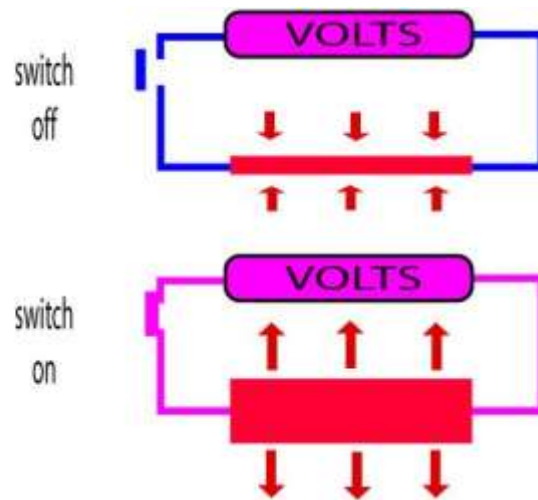


Figure 2.4: Piezo Electric Crystal [63]

In an ultrasound examination, a transducer both sends the sound waves and receives the echoing waves. When the transducer is pressed against the skin, it directs small pulses of inaudible, high-frequency sound waves into the body. As the sound waves bounce off internal organs, fluids and tissues, the sensitive microphone in the

transducer records tiny changes in the sound's pitch and direction. These signature waves are instantly measured and displayed by a computer, which in turn creates a real-time picture on the monitor. One or more frames of the moving pictures are typically captured as still images. Small loops of the moving real-time images may also be saved.



Figure 2.5: Working Method of Ultrasound Examination (Part-1) [63]

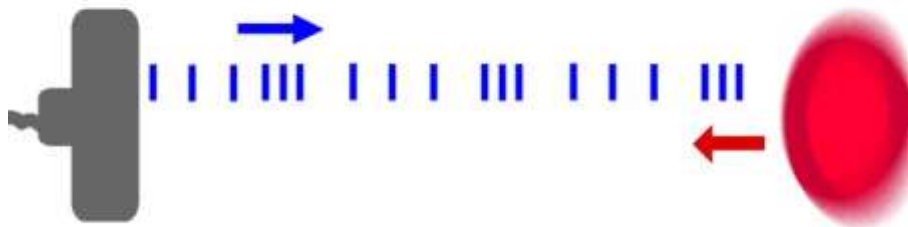


Figure 2.6: Working Method of Ultrasound Examination (Part-2) [63]

Doppler ultrasound, a special application of ultrasound, measures the direction and speed of blood cells as they move through vessels. The movement of blood cells causes a change in pitch of the reflected sound waves (called the Doppler effect). A computer collects and processes the sounds and creates graphs or color pictures that represent the flow of blood through the blood vessels.

## 2.3 Ultrasound Wavelength and Frequency

The wavelength and frequency of US are inversely related, i.e., ultrasound of high frequency has a short wavelength and vice versa. US waves have frequencies that exceed the upper limit for audible human hearing, i.e., greater than 20 kHz.<sup>3</sup> Medical ultrasound devices use sound waves in the range of 1–20 MHz. Proper selection of transducer frequency is an important concept for providing optimal image resolution in diagnostic and procedural US. High-frequency ultrasound waves (short wavelength) generate images of high axial resolution. Increasing the number of waves of compression and rarefaction for a given distance can more accurately discriminate between two separate structures along the axial plane of wave propagation. However, high-frequency waves are more attenuated than lower frequency waves for a given distance; thus, they are suitable for imaging mainly superficial structures.<sup>5</sup> Conversely, low-frequency waves (long wavelength) offer images of lower resolution but can penetrate to deeper structures due to a lower degree of attenuation (Figure 2.6). For this reason, it is best to use high-frequency transducers (up to 10–15 MHz range) to image superficial structures (such as for stellate ganglion blocks) and low-frequency transducers (typically 2–5 MHz) for imaging the lumbar neuraxial structures that are deep in most adults (Figure 2.7). Ultrasound waves are generated in pulses (intermittent trains of pressure) that commonly consist of two or three sound cycles of the same frequency (Figure 2.8).

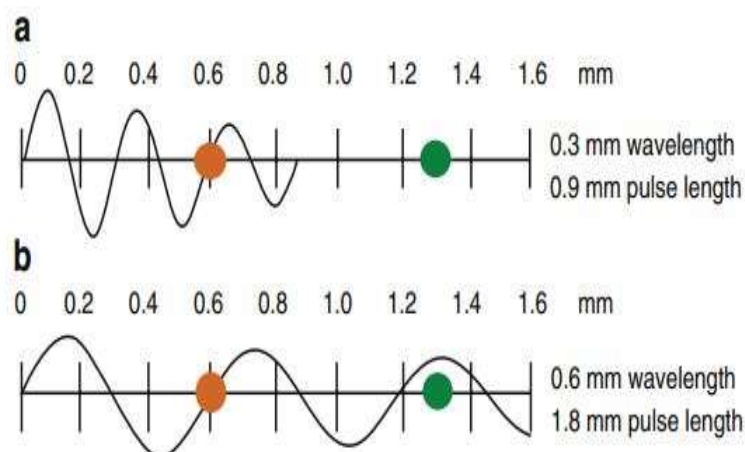


Figure 2.7: Attenuation of ultrasound waves and its relationship to wave frequency. Note that higher frequency waves are more highly attenuated than lower frequency waves for a given distance. Reproduced with permission from ref. [64]

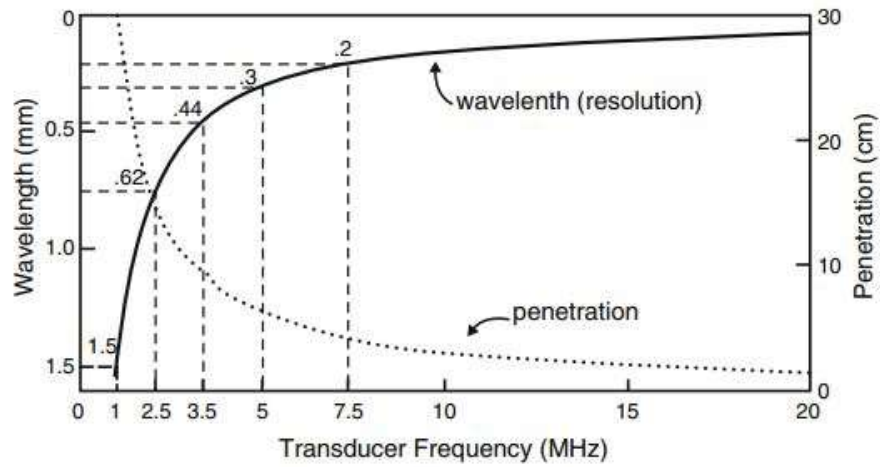


Figure 2.8: A comparison of the resolution and penetration of different ultrasound transducer frequencies. This figure was published in ref. [64] Copyright Elsevier (2000).

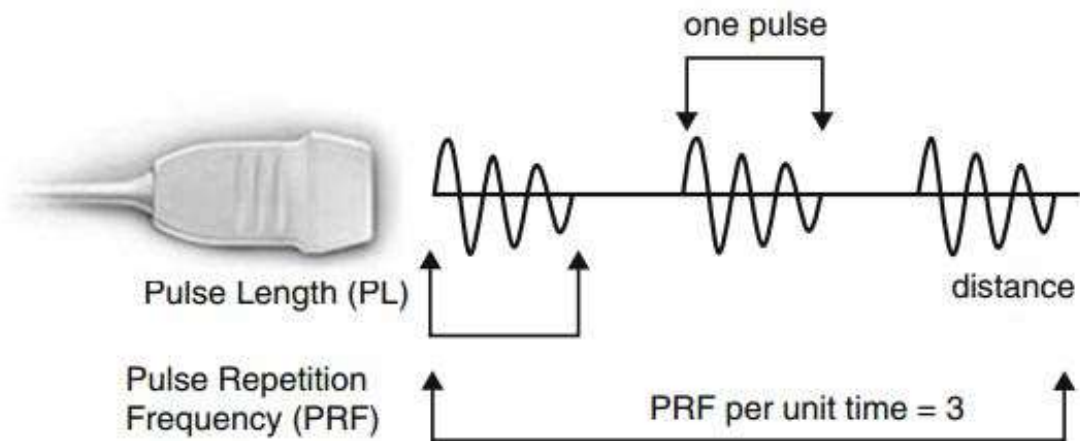


Figure 2.9: Schematic representation of ultrasound pulse generation. Reproduced with permission from ref [64]



The pulse repetition frequency (PRF) is the number of pulses emitted by the transducer per unit of time. Ultrasound waves must be emitted in pulses with sufficient time in between to allow the signal to reach the target of interest and be reflected back to the transducer as echo before the next pulse is generated. The PRF for medical imaging devices ranges from 1 to 10 kHz.

Resolution is the ability to see two things as two things. If the resolution is good, the picture will be clear and the two objects will look like two objects. If the resolution is poor, the picture will be blurred and the two objects will look like one. Our aim is to get the best possible resolution from our ultrasound machine. Higher the resolution, higher will be the quality of the image we see.

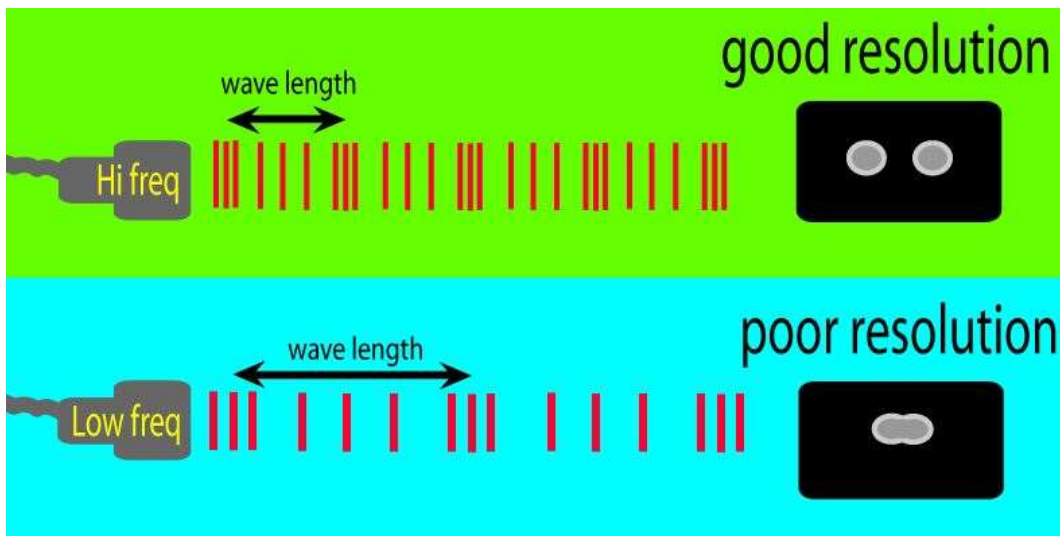


Figure 2.10: Ultrasound Wavelength and Frequency [63]

## 2.4 Ultrasound–Tissue Interaction

As US waves travel through tissues, they are partly transmitted to deeper structures, partly reflected back to the transducer as echoes, partly scattered, and partly transformed to heat. For imaging purposes, we are mostly interested in the echoes reflected back to the transducer. The amount of echo returned after hitting a tissue interface is determined by a tissue property called acoustic impedance. This is an intrinsic physical property of a medium defined as the density of the medium times the velocity of US wave propagation in the medium.

Table 2.1: Acoustic impedances of different body tissues and organs.

Body Tissue	Acoustic impedance ( $10^6$ Rayls)
Air	0.0004
Lung	0.18
Fat	1.34
Liver	1.65
Blood	1.65
Kidney	1.63
Muscle	1.71
Bone	7.8

Reproduced with permission from ref [64]

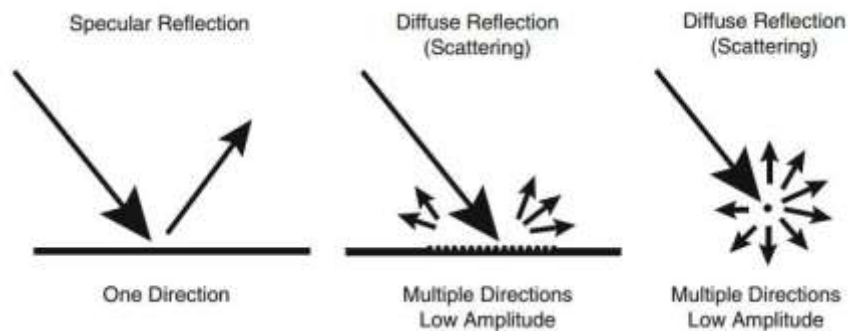


Figure 2.11: Different types of ultrasound wave–tissue interactions. Reproduced with permission [64]

Air-containing organs (such as the lung) have the lowest acoustic impedance, while dense organs such as bone have very high-acoustic impedance (Table 2.1). The intensity of a reflected echo is proportional to the difference (or mismatch) in acoustic impedances between two mediums. If two tissues have identical acoustic impedance, no echo is generated. Interfaces between soft tissues of similar acoustic impedances usually generate low-intensity echoes. Conversely interfaces between soft tissue and bone or the lung generate very strong echoes due to a large acoustic impedance gradient.<sup>7</sup> When an incident ultrasound pulse encounters a large, smooth interface of two body tissues with different acoustic impedances, the sound energy is reflected back to the transducer. This type of reflection is called specular reflection, and the echo intensity generated is proportional to the acoustic impedance gradient between the two mediums (Figure 2.10). A soft-tissue–needle interface when a needle is inserted “in-plane” is a good example of specular reflection. If the incident US beam reaches the linear interface at  $90^\circ$ , almost all of the generated echo will travel back to the transducer. However, if the angle of incidence with the specular boundary is less than  $90^\circ$ , the echo will not return to the transducer, but rather be reflected at an angle equal to the angle of incidence (just like visible light reflecting in a mirror). The returning echo will potentially miss the transducer and not be detected. This is of practical importance for the pain physician, and explains why it may be difficult to image a needle that is inserted at a very steep direction to reach deeply located structures. Refraction refers to a change in the direction of sound transmission after hitting an interface of two tissues with different speeds of sound transmission. In this instance, because the sound frequency is constant, the wavelength has to change to accommodate the difference in the speed of sound transmission in the two tissues. This results in a redirection of the sound pulse as it passes through the interface. Refraction is one of the important causes of incorrect localization of a structure on an ultrasound image. Because the speed of sound is low in fat (approximately 1,450 m/s) and high in soft tissues (approximately 1,540 m/s), refraction artifacts are most prominent at fat/soft tissue interfaces.

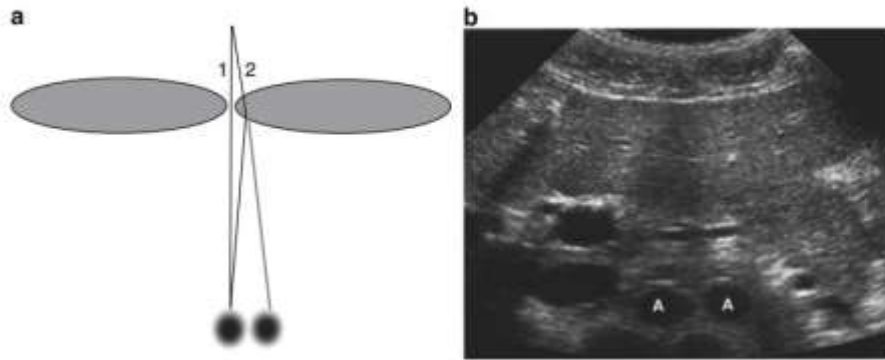


Figure 2.12: Refraction artifact. Diagram (a) shows how sound beam refraction results in duplication artifact. (b) is a transverse midline view of the upper abdomen showing duplication of the aorta (A) secondary to rectus muscle refraction. This figure was published in ref. [65] Copyright Elsevier (2004).

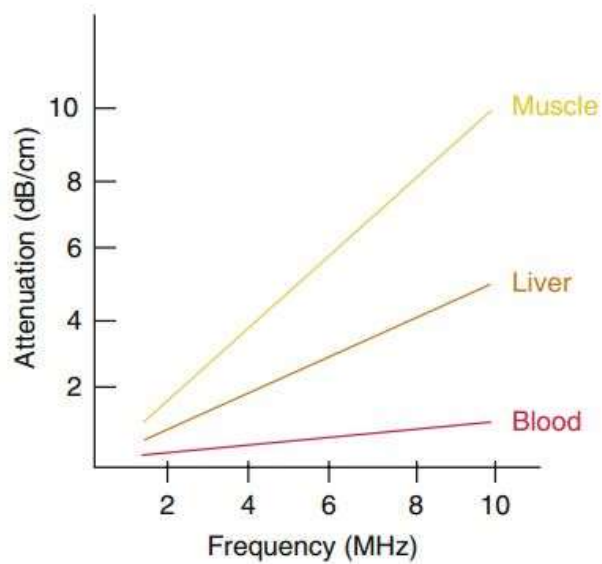


Figure 2.13: Degrees of attenuation of ultrasound beams as a function of the wave frequency in different body tissues. Reproduced with permission from ref. [64]

The most widely recognized refraction artifact occurs at the junction of the rectus abdominis muscle and abdominal wall fat. The end result is duplication of deep abdominal and pelvic structures seen when scanning through the abdominal midline (Figure 2.11). Duplication artifacts can also arise when scanning the kidney due to refraction of sound at the interface between the spleen (or liver) and adjacent fat. [65] If the ultrasound pulse encounters reflectors whose dimensions are smaller than the ultrasound wavelength, or when the pulse encounters a rough, irregular tissue interface, scattering occurs. In this case, echoes reflected through a wide range of angles result in reduction in echo intensity. However, the positive result of scattering is the return of some echo to the transducer regardless of the angle of the incident pulse. Most biologic tissues appear in US images as though they are filled with tiny scattering structures. The speckle signal that provides the visible texture in organs like the liver or muscle is a result of interface between multiple scattered echoes produced within the volume of the incident ultrasound pulse. [66]

As US pulses travel through tissue, their intensity is reduced or attenuated. This attenuation is the result of reflection and scattering and also of friction-like losses. These losses result from the induced oscillatory tissue motion produced by the pulse, which causes conversion of energy from the original mechanical form into heat. This energy loss to localized heating is referred to as absorption and is the most important contributor to US attenuation. Longer path length and higher frequency waves result in greater attenuation. Attenuation also varies among body tissues, with the highest degree in bone, less in muscle and solid organs, and lowest in blood for any given frequency (Figure 2.12)

# Chapter 3

## Current State of Art

### 3.1 Introduction

Ultrasound (US) images have been widely used in the diagnosis of breast cancer in particular. While experienced doctors may locate the tumor regions in a US image manually, it is highly desirable to develop algorithms that automatically detect the tumor regions in order to assist medical diagnosis.

Ultrasound images are difficult to segment due to presence of speckle noise and the boundaries of abnormal regions are also difficult to recognize due to similarity. It is important to segment the image for correct and effective diagnosis. Manual method of segmentation is good but not effective for segmentation of large data sets, due to this an automatic or computerized segmentation is motivated.

So, early detection and diagnosis is very important for breast cancer. Currently, breast ultrasound (BUS) imaging is a valuable method in early detection and classification of breast lesions [11].

In present world, researcher working on different types of segmentation for breast ultrasound (BUS) image processing.

### 3.2 Segmentation

Segmentation is one of the-bottlenecks of many image analysis and computer vision tasks ranging from medical image processing to robot navigation. Most of the further analysis relies on the results of the segmentation procedure, and accurate extraction of clinical information from medical images promises reliability for clinical applications and it is the basis of 3-D model reconstruction. But image segmentation

is a very difficult problem in practice. Standard image processing techniques fail to deliver satisfying results for most medical applications. So far no one algorithm can robustly segment a variety of relevant structure in medical images over a range of datasets [12].

The principal segmentation challenges pertain to characterizing the textured appearance and geometry of a cancer relative to normal tissue, and accommodating artifacts such as the possibly strong attenuation across an image and shadowing, as well as the “fuzziness” of cancerous mass boundaries which makes border delineation difficult. Importantly, the studies of Stavos [13] - [15] have greatly influenced the design of algorithms for breast mass detection. Interestingly, no significant work has looked at the screening case, i.e., most work has assumed the presence of a, typically single, suspicious mass. Many techniques have been developed for BUS segmentation. They are categorized into histogram thresholding, region growing, model-based (active contour, level set, Markov random field) and machine learning. Simple histogram thresholding [16, 17] or region-growing algorithms [18, 19] can find the preliminary lesion boundary. In a histogram thresholding method, an intensity threshold is chosen at the valley of the image histogram to separate the image into background and foreground. For a region growing method, a region is grown from the seed point (start point) by adding similar neighboring pixels.

Although efficient, these methods cannot generate a precise boundary because their over-simplified concepts and the high sensitivity to noise. However, they can serve as an intermediate step to provide a rough contour [20] or can be combined with post-processing procedures such as morphological operations [21, 22, 23], disk expansion [24], Bayesian neural network [25], function optimization [44] etc. Horsch et al. [26] presented a method involving thresholding a preprocessed image that has enhanced mass structures. Comparison is made of a partially automatic and fully automatic version of the method with manual delineation on 400 cases/757 images (124 “complex” cysts, 182 benign masses, and 94 malignant masses). They compute four image based features (shape, echogenicity, margin, and posterior acoustic behavior) defined respectively in terms of the depth-to-width ratio, autocorrelation, “normalized radial gradient,” and comparison of gray levels, to test their effectiveness at distinguishing malignant and benign masses. This method was further evaluated in [27] and [28] to assess the advantages of different features using linear discriminant analysis where the best two features were found to be the depth-to-width ratio (shape) and normalized radial gradient (margin). In later work aimed at further automating the method Drukker et al. [29] extended this work to include mass detection by proposing to first filter the

images with a radial gradient index filtering technique. The method was tested on the same database as in [27] and [28]. They showed that 75% of lesions were correctly identified.

Neural network (NN) based methods have proved to be popular in this area. These aim to make a classification decision based on a set of input features. For instance, Chen et al. [30] presented a NN approach where input features were variance contrast, autocorrelation contrast, and the distribution distortion in the (Daubechies) wavelet coefficients and a multilayered perceptron (MLP) neural network with one hidden layer was trained by error back propagation. The method was applied to a database of 242 cases (161 benign, 81 carcinoma) giving a sensitivity of 98.77% and specificity of 81.77%. They strongly argued that image texture was an important component that made their method successful.

Huang and Chen [31] proposed an approach that integrates the advantages of NN classification and a watershed segmentation methods to extract contours of a breast tumor from ultrasound images. The main novelty of this work is in the preprocessing step which helps effectively the watershed algorithm by means of a reasonably good selection of markers. The authors proposed to use a self-organizing map (SOM) texture based NN in order to select adaptively (i.e., locally) from a set of nine pre-defined filters the appropriate preprocessing filter to use. Their method was tested on a database of 60 images (21 benign, 39 carcinomas), 40 used for training, 20 for testing. Measures of contour difference and area difference between the method and manual delineation were evaluated although strong conclusions cannot be drawn from this evaluation.

Xiao et al. [32] presented an expectation maximization method that simultaneously estimates the attenuation field at the same time as classification of regions into different (intensity based) regions. The number of regions (classes) needs to be specified, which in the intended application is not a strong limitation. That method was tested on experimental data with different time gain compensation (TGC) settings to show that their approach gave consistent segmentations under different TGC settings but has not undergone a large clinical assessment. This method is compared to that of Boukerroui in [33].

Madabhushi and Metaxas [34] combined intensity, texture information, and empirical domain knowledge used by radiologists with a deformable shape model in an attempt to limit the effects of shadowing and false positives. Their method requires training but in the small database. Using manual de-lination



of the mass by a radiologist as a reference, and the Hausdorff distance and average distance as boundary error metrics, they showed that their method is independent of the number of training samples, shows good reproducibility with respect to parameters, and gives a true positive area of 74.7%. They also argued that it has automation advantages over the work of Horsch et al. [27].

Boukerroui et al. [35] used a Markov random field to model the region process and to focus on the adaptive characteristics of the algorithm. Their method introduced a function to control the adaptive properties of the segmentation process, and took into account both local and global statistics during the segmentation process. A new formulation of the segmentation problem was utilized to control the effective contribution of each statistical component. The merit of MRF modeling is that it provides a strong exploitation of the pixel correlations. The segmentation results can be further enhanced via the application of maximum a posteriori segmentation estimation scheme based on the Bayesian learning paradigm.

Watershed based approaches have shown promising performances for ultrasound image segmentation. The methods consider image as topographic surface wherein the grey level of a pixel is interpreted as its altitude. Water flows along a path to finally reach a local minimum. The biggest challenge for such methods is over segmentation; to address the problem; many approaches have been proposed and can be categorized into two types: marker controlled and cell competition.

Marker controlled methods inundate the gradient landscape of image and define watersheds when the flooding of distinct markers rendezvous with each other. Hence, the identification of markers is very crucial in solving the over segmentation problem. The method proposed in [36] was a texture-based approach that selected the marker candidates as seeds for the water level immersion. A self-organization map was trained to identify the texture of lesions as the flooding markers. Distinctively, the method in [37] adopted a thresholding and morphological operation scheme to seek flooding markers. It required a heuristic estimation of the best thresholding of markers to achieve the task of lesion delineation. Cell competition approaches, on the other hand, alleviate the over segmentation problem in a different way. A two-pass watershed transformation [38] was performed to generate the cell tessellation on the original ultrasound image or ROI. In this method, a competition scheme based on the cell tessellation was carried out by allowing merge and split operations of cells. The cost function was devised to characterize boundary saliency and regional homogeneity of an image partition, and it drove the

competition process to converge to a prominent component structure. However, neither marker controlled nor cell competition approaches guarantee to solve the over segmentation problem completely [39].

Although some of the previous methods can be applied in 3-D, the literature on 3-D is less extensive. For instance, Chen et al. [40], Chang et al.[41]–[43], and Sahiner et al.[44] take a deformable active contour approach. Chang et al. [45] applied an active contour which uses intensity and intensity variance information. The method was tested on eight tumors (four benign, four malignant) with volume estimates compared with estimates by manual delineations. Using the match rate as a performance metric, the average match rate was about 95%. Sahiner et al. [46] compared 2-D and 3-D intensity gradient active contour segmentation based methods, the active contour initialized by hand, and with algorithm parameters determined empirically. Having found the segmentation solution, depth-to-width ratio, a posterior shadowing feature measure, and 72 texture features based on co-occurrence matrix analysis were computed around the boundary for each 2-D slice and linear discriminant analysis used to classify volumes. Four radiologists graded the volumes in terms of perceived malignancy on a scale 1–10. They showed that the radiologist and computer based methods were not statistically different in classification (versus average for radiologists). However, they did not look at the accuracy of segmentation in depth and recognized that this was an area of possible improvement.

# Chapter 4

## Segmentation Methods

### 4.1 Introduction

There are many types of segmentation methods for ultrasound image processing. From those few are popular. Popular segmentations methods are-

- Watershed segmentation.
- Region Based segmentation (region growing, level set).
- Histogram thresholding (global, local thresholding).
- Model-based (active contour, marker random field).
- Machine Learning.
- Segmentation based on clustering (Hard, K-means, fuzzy clustering).

### 4.2 Explanation of different kinds of segmentation

#### 4.2.1 Watershed segmentation

In the study of image processing a watershed of a grayscale image is analogous to the notion of a catchment basin of a height map. In short, a drop of water following the gradient of an image flows along a path to finally reach a local minimum. Intuitively, the watershed of a relief corresponds to the limits of the adjacent catchment basins of the drops of water.

There are different technical definitions of a watershed. In graphs, watershed lines may be defined on the nodes, on the edges, or hybrid lines on both nodes and edges. Watersheds may also be defined in the continuous domain [47]. There are also many different algorithms to compute watersheds. Watershed algorithm is used in image processing primarily for segmentation purposes.

## **4.2.2 Region Based Segmentation**

Region based segmentation [48] is based on partitioning an image into regions. Homogeneous regions are found based on the intensity value or texture feature. Its aim is to characterize the detected objects by parameter analysis (shape, size, position etc.). The best known region based category is split and merge algorithm. Boundary based method [49] overcome the pitfalls of region based segmentation. This method is used for searching implicit and explicit boundaries between regions which are correlated with different types of tissues.

Edge detection is the standard category of boundary based method. The hybrid technique [50] is a combination of both boundaries based method and region based segmentation method. In active contour method [51] of segmentation technique, objects are detected using techniques of curve growth. This method is used to detect the edges of regions in image in which gray scale intensities are different with respect to surrounding region.

## **4.2.3 Histogram Thresholding**

In thresholding based method of segmentation [52], no spatial information of pixels is examined. Gray-level image is converted into a binary image in thresholding. In ultrasound images, noise and boundaries of abnormal regions are not handled well in this segmentation technique.

## **4.2.4 Model-based (active contour, marker random field)**

Active contour models have been extensively applied to image segmentation for the past years. It was introduced by Kass for segmenting objects in images using dynamic curves [53]. Active contour models are also called snakes. Generally speaking, snakes can achieve a smooth and closed contour as well as sub-pixel accuracy. But it also has disadvantages, for example, it cannot change topology and the initial contour must be close to the object boundary. In 1988, Osher and Sethian proposed level set method which can solve the problems caused by snakes [54]. The curve evolution combining active contour models with level set method is widely applied in the segmentation. However, during the evolution of level set, it is numerically necessary to keep the evolving level set function close to a signed distance function.

## **4.2.5 Machine Learning**

Imaging technologies have influenced biology and neuro-science profoundly, starting from the cell theory and the neuron doctrine. Today's golden age of fluorescent probes has renewed the belief that innovations in microscopy lead to new discoveries. But much of the excitement over imaging overlooks an important technological gap: scientists not only need machines for making images, but also machines for seeing them.

With today's automated imaging systems, it is common to generate and archive torrents of data. For some experiments, the greatest barrier is no longer acquiring the images, but rather the labor required to analyze them. Ideally, computers would be made smart enough to analyze images with little or no human assistance. This is easier said than done — it involves fundamental problems that have eluded solution by researchers in artificial intelligence for half a century.

One of these problems is image segmentation, the partitioning of an image into sets of pixels (segments) corresponding to distinct objects. For example, a digital camera user might like to segment an image of a room into people, pieces of furniture, and other household objects. A radiologist may need the shapes and sizes of organs in an MRI or CT scan. A biologist may want to find the cells in a fluorescence image from a microscope. Engineers have tried to make computers perform all of these tasks, but computers still make many more errors than humans.

## **4.2.6 Segmentation based on clustering (Hard, K-means, fuzzy clustering)**

One natural view of segmentation is that we are attempting to determine which components of a data set naturally “belong together”. This is a problem known as clustering; there is a wide literature. Generally, we can cluster in two ways:

Partitioning: here we have a large data set, and carve it up according to some notion of the association between items inside the set. We would like to decompose it into pieces that are “good” according to our model. For example, we might:

- decompose an image into regions which have coherent colour and texture inside them;
- take a video sequence and decompose it into shots — segments of video showing about the same stuff from about the same viewpoint;
- decompose a video sequence into motion blobs, consisting of regions that have coherent colour, texture and motion.

Grouping: here we have a set of distinct data items, and wish to collect sets of data items that “make sense” together according to our model. Effects like

occlusion mean that image components that belong to the same object are often separated. Examples of grouping include:

- collecting together tokens that, taken together, forming an interesting object
- collecting together tokens that seem to be moving together.

# Chapter 5

## Watershed Segmentation

### 5.1 Introduction

The watershed transform is the method of choice for image segmentation in the field of mathematical morphology. In gray scale mathematical morphology, the watershed transform, originally proposed by Digabel and Lantuejoul [55], is the method of choice for image segmentation. The intuitive idea underlying this method comes from geography: It regards the gradient magnitude image as a landscape where the intensity values correspond to the elevation.

Morphological segmentation is an image plugin that combines morphological operations, such as extended minima and morphological gradient, with watershed flooding algorithms to segment grayscale images of any type in 2D and 3D.

In geography, a watershed is the ridge line that divides areas drained by different river systems. A catchment basin is the geographical area draining into a river or reservoir. To understand watershed, transform basically we have to view it as a topological surface.

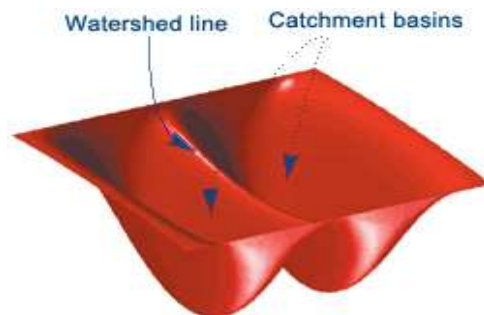


Figure 5.1: Topographic Relief Image [60]



It is especially useful for segmenting object that are touching one another. Otherwise the reference image comes to as a single foreground.

## 5.2 Basic Algorithm

- Suppose, a hole is punched at each regional local minimum and the entire topography is flooded from below by letting the water rise through the holes at uniform rate.
- Pixels below the water level at a given time are managed as flooded.
- When we raise the water level incrementally, the flooded regions will grow in size.
- Eventually, the water will rise to a level where two flooded regions from separate catchment basins will merge.
- When this occurs, the algorithm constructs a one-pixel thick dam that separates the two regions.
- The flooding continues until the entire image is segmented into catchment basins divided by watershed ridge line.

## 5.3 Implementation

Different kinds of approach are being needed to implement the watershed transform. The watershed segmentation can be done by-

- Using the distance transform
- Using gradients
- Marker-controlled

## 5.3.1 The Distance Transform

The distance transform is the common tool in conjunction with the watershed transform. Actually, it is the distance from every pixel to the nearest nonzero-valued pixel.

It can be calculated in different way. Such as-

i) Euclidian Distance:

In mathematics, the Euclidean distance or Euclidean metric is the "ordinary" (i.e. straight-line) distance between two points in Euclidean space. With this distance, Euclidean space becomes a metric space. The associated norm is called the Euclidean norm. Older literature refers to the metric as Pythagorean metric. A generalized term for the Euclidean norm is the L2 norm or L2 distance.

The distance between two points defined as the square root of the sum of the squares of the differences between the corresponding coordinates of the points; for example, in two-dimensional Euclidean geometry, the Euclidean distance between two points  $\mathbf{a} = (\mathbf{a}_x, \mathbf{a}_y)$  and  $\mathbf{b} = (\mathbf{b}_x, \mathbf{b}_y)$  is defined as:

$$d(\mathbf{a}, \mathbf{b}) = \sqrt{(\mathbf{a}_x - \mathbf{b}_x)^2 + (\mathbf{a}_y - \mathbf{b}_y)^2} \text{-----5.1}$$

ii) City Block Distance

It is also known as Manhattan distance, boxcar distance, absolute value distance. It represents distance between points in a city road grid. It examines the absolute differences between coordinates of pair of objects.

$$d_{ij} = \sum_{k=1}^x |X_{ij} - X_{jk}| \text{-----5.2}$$

### iii) Chessboard Distance

In mathematics, Chebyshev distance (or Tchebychev distance), maximum metric, or  $L_\infty$  metric [56] is a metric defined on a vector space where the distance between two vectors is the greatest of their differences along any coordinate dimension [57]. It is named after Pafnuty Chebyshev.

It is also known as chessboard distance, since in the game of chess the minimum number of moves needed by a king to go from one square on a chessboard to another equals the Chebyshev distance between the centers of the squares, if the squares have side length one, as represented in 2-D spatial coordinates with axes aligned to the edges of the board [58].

The Chebyshev distance between two vectors or points  $p$  and  $q$ , with standard coordinates  $p_i$  and  $q_i$ , respectively, is

$$D_{\text{Chebyshev}}(p, q) := \max_i (|p_i - q_i|). \text{-----}5.3$$

## 5.3.2 Gradients

For watershed segmentation gradient magnitude is often used. The gradient magnitude has high pixel values along object edges, and low pixel values everywhere else. It has problems. Due to this over segmentation occurred. Another thing is too many ridge lines that do not correspond to the object boundaries of interest.

## 5.3.3 Marker-Controlled

A marker is a connected component belonging to an image. A set of internal markers that are inside each of the objects of interest. And a set of external markers that are

contained in the background. Various kind of methods such as linear filtering, nonlinear filtering and morphological processing. It has also problems. Severely segmented, due in part to the large number of regional minima.

Algorithm by using Marker-Controlled Watershed Segmentation

Segmentation using the watershed transform works better if you can identify, or "mark," foreground objects and background locations.

Marker-controlled watershed segmentation follows this basic procedure:

- Compute a segmentation function. This is an image whose dark regions are the objects you are trying to segment.
- Compute foreground markers. These are connected blobs of pixels within each of the objects.
- Compute background markers. These are pixels that are not part of any object.
- Modify the segmentation function so that it only has minima at the foreground and background marker locations.
- Compute the watershed transform of the modified segmentation function.



Figure 5.2: Original Image [61]

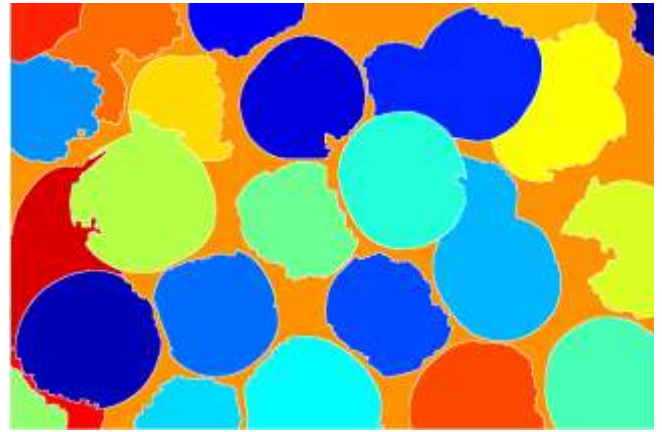


Figure 5.3: Colored watershed label matrix (Lrgb) [61]

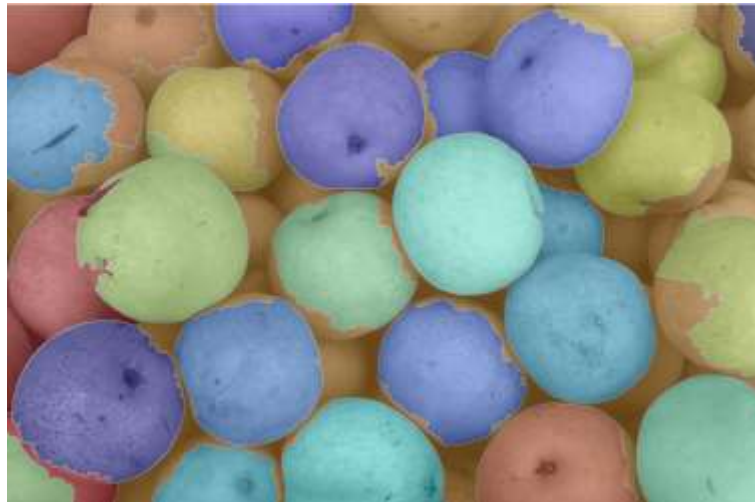


Figure 5.4: Lrgb superimposed transparently on original image [61]

Here, we used a technique for watershed segmentation which is described below.

Step 1:

We took a ROI image as our reference image.

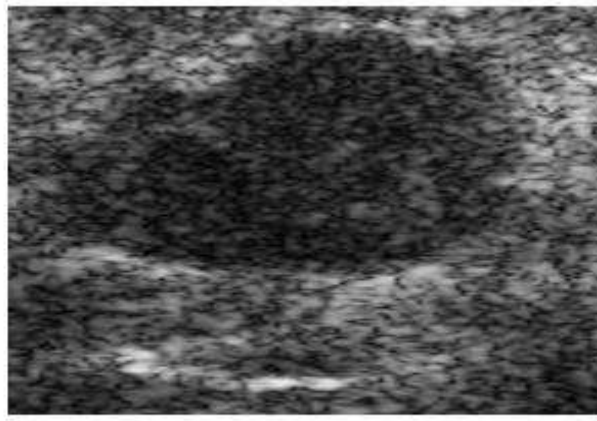


Figure 5.5: Ultrasound Image (Original Image)

Step 02:

Then we transformed the ROI image into watershed RGB image.

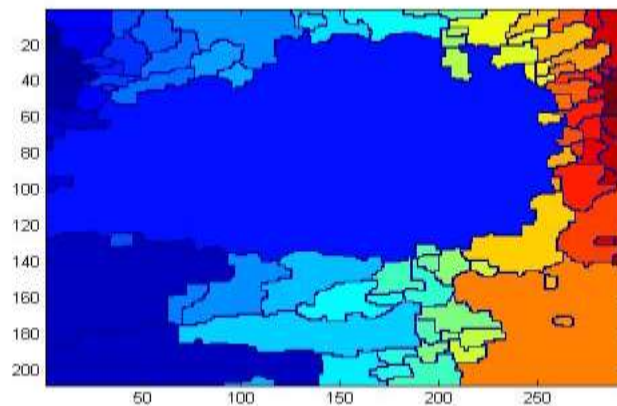


Figure 5.6: Watershed RGB Image

Forming binary image by preserving the largest connected area in the watershed image. We observed the large connected component of watershed image is our desired lesion. Therefore, we followed the following principle to form the binary image:

- Ranked all the segmented region of the watershed image based on area
- Formed binary image by preserving the largest connected area in the watershed image.

Thus we get a binary image having only our lesion. Fig 5.7 shows the binary image.

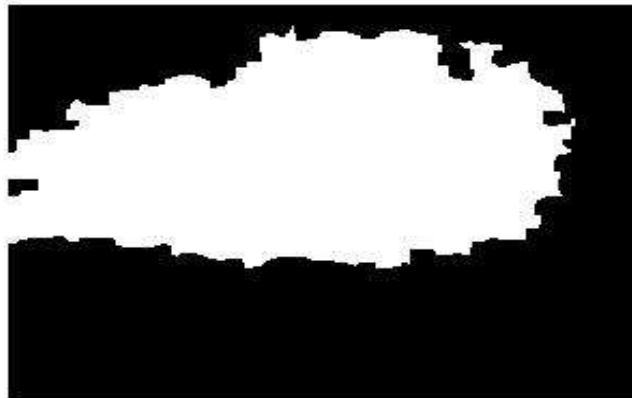


Figure 5.7: Binary Thresholding Image

Step 04:

Sobel Edge Detection

The Sobel operator, sometimes called the Sobel-Feldman operator or Sobel filter, is used in image processing and computer vision, particularly within edge detection algorithms where it creates an image emphasizing edges.

The gradient of the image is calculated for each pixel position in the image.

The steps of SOBEL edge detection are:

- It uses a 3x3 filter mask to calculate gradient in every pixel location of the input image.

X1	X2	X3
X4	X5	X6
X7	X8	X9

Figure 5.8: 3×3 Image Neighborhood

The Magnitude of the vector  $\Delta f$  is denoted as,

$$\Delta f = \max (\Delta f) = \left[ G_x^2 + G_y^2 \right]^{\frac{1}{2}} \text{-----5.4}$$

Where  $G_x$  is for x direction and  $G_y$  for y direction.

The sobel masks (3×3):

For x-Direction:

$$\begin{matrix} -1 & -2 & -1 \\ 0 & 0 & 0 \\ 1 & 2 & 1 \end{matrix}$$

For y-Direction:

$$\begin{matrix} -1 & 0 & 1 \\ -2 & 0 & 2 \\ -1 & 0 & 1 \end{matrix}$$



Find the x-direction derivative: Subtract the first row from the third row using the mask.

$$G_x = (X_7 + 2X_8 + X_9) - (X_1 + 2X_2 + X_3) \text{ -----} 5.5$$

Find the y-direction derivative: Subtract the first row from the third row using the mask.

$$G_y = (X_3 + 2X_6 + X_9) - (X_1 + 2X_4 + X_7) \text{ -----} 5.6$$

Find the gradient:

$$G_x^2 \text{ \& } G_y^2$$

Then find  $\Delta f$  using above law.

The procedure is done for the whole image matrix.

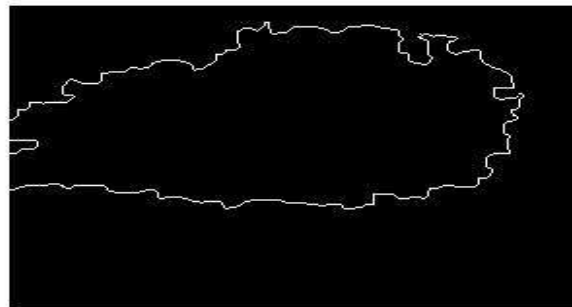


Figure 5.9: After Sobel Edge Detection

Segmented Image

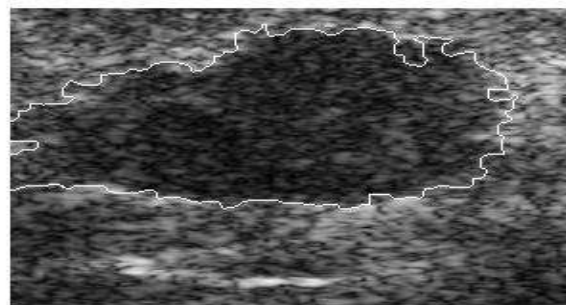


Figure 5.10: Segmented Image (Superimposed into original image)

We applied the above technique in different kinds of ultrasound images which is given below:

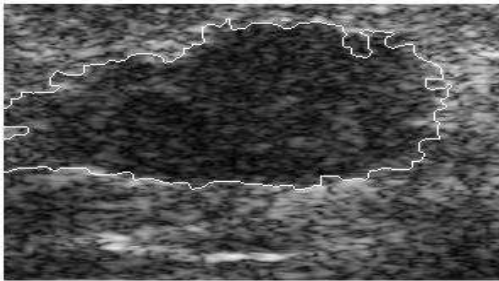


Figure 5.11: Segmented Image (Type 1)

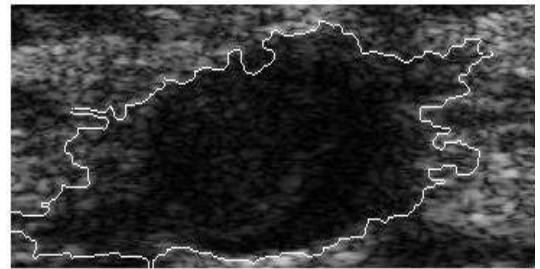


Figure 5.12: Segmented Image (Type 2)

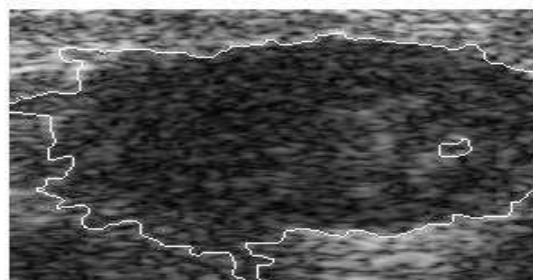


Figure 5.13: Segmented Image (Type 3)

# Chapter 6

## Region Growing Segmentation

### 6.1 Introduction

Region growing is a procedure that group's pixels in whole image into sub regions or larger regions based on predefined Criterion. It has many advantage. These are:

- It is easy to construct regions from their borders and it is easy to detect borders of existing regions.
- Combination of results may often be a good idea.
- Homogeneity of regions is used as the main segmentation criterion in region growing.
- Region growing methods can provide the original images which have clear edges with good segmentation results.

Region growing segmentation is two types. Those are:

Edge-based segmentation: borders between regions

Region-based segmentation: direct construction of regions

It is easy to construct regions from their borders and it is easy to detect borders of existing regions. Segmentations resulting from edge-based methods and region growing methods are not usually exactly the same. Combination of results may often be a good idea. Region growing techniques are generally better in noisy images where edges are extremely difficult to detect. Homogeneity of regions is used as the main segmentation criterion in region growing.

The criteria for homogeneity:

- gray level
- color, texture
- shape
- model

etc.

Resulting regions of the segmented image must be both homogeneous and maximal.

Algorithm for region growing method:

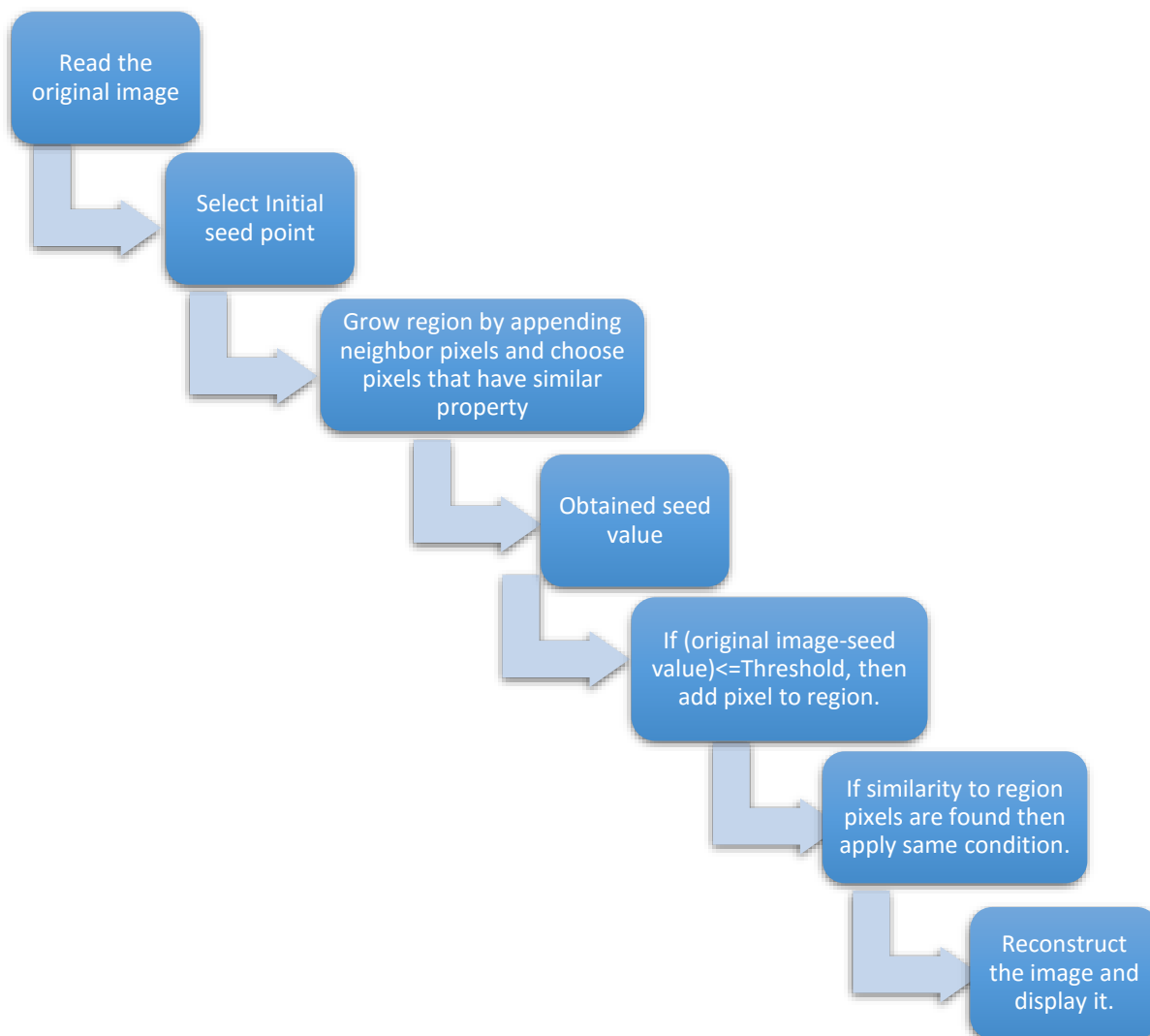


Figure 6.1: Flowchart of region growing algorithm

Process:

Step 01:

Original Image

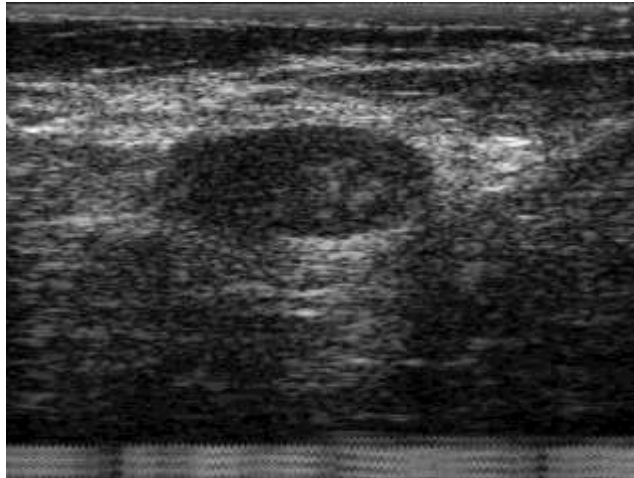


Figure 6.2: BUS Image

Step 02:

Seed Selection

Here we represent seed by  $3 \times 3$  matrix.

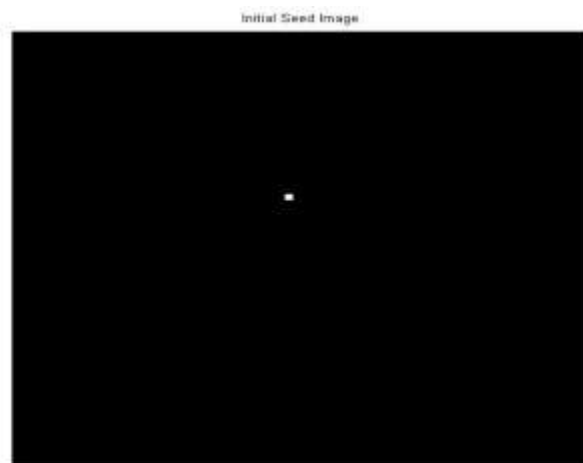


Figure 6.3: Seed selection

## Separations of regions by region growing

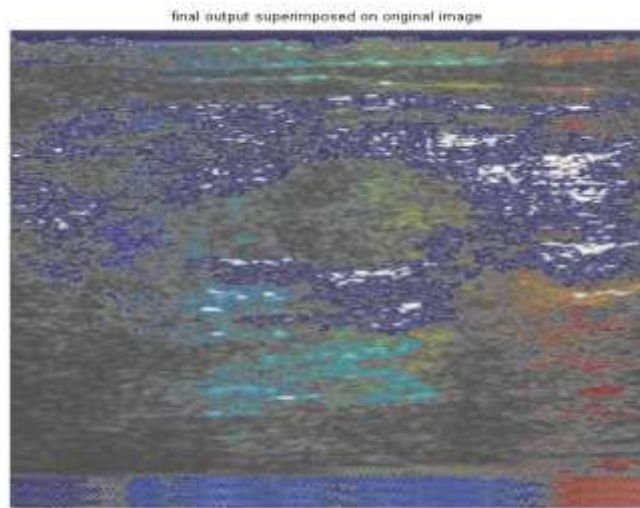


Figure 6.4: Applying region growing algorithm

Step 04:

Segmented Image



Figure 6.5: Segmented Image

Step 05:

Horizontal cut based entropy filtering

We first applied entropy filtering on BUS image. Entropy is a textural feature and can be defined as a measure of randomness:

$$\text{Entropy} = - \sum_{i=0}^{L-1} p(x_i) \log_2 p(x_i) \text{ -----6.1}$$

In above equation

x is a random variable

p(x) is the histogram of the intensity levels

L is the number of possible intensity levels.

From the entropy filtered images, we observed that the entropy values are different for different regions. We categorized entropy values based on these regions. These values are tabulated in Table 6.1.

Regions (in terms of location)	Regions (in terms of echogenicity)	Entropy Value	Comments
Boundary of the lesion	Hyperechoic	>6.5	This is general for all test images
Inside the lesion	Anechoic	5~6	Varies with images but mostly the entropy value is lesser than the values around the lesion
Rest of the image	Mostly hypoechoic	5~6.5	With some anechoic regions

The entropy values in the dark (anechoic) region inside the lesion vary from 3 to 5. The white (hyperechoic) region found near the boundary of the lesion has very high entropy values ranging from 6 to 7.5. The rest of the image with mostly gray regions (hypoechoic) has values from 5 to 6.5. The regions can be seen in the original BUS image shown in Fig. 6.1. Corresponding entropy image in Fig. 6.2. Low entropy values indicate that randomness is small inside the lesion, i.e. the grayscale-intensity values within the lesion do not vary much compared to that of the region near boundary. Due to high variation of grayscale-intensity values, entropy is higher near boundary. These echogenic regions are depicted in Fig 6.6 and Fig 6.7. We used this information for our horizontal cut.

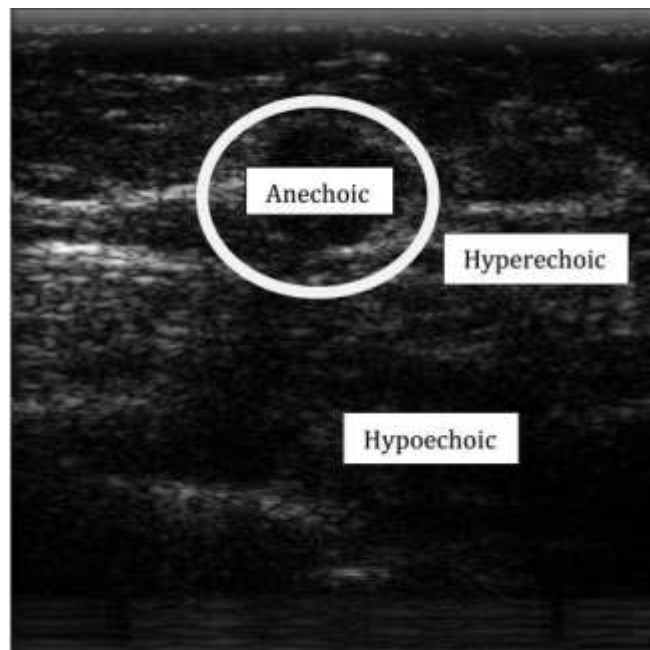


Figure 6.6: Original BUS image showing echogenicity



This method we applied in our segmented image

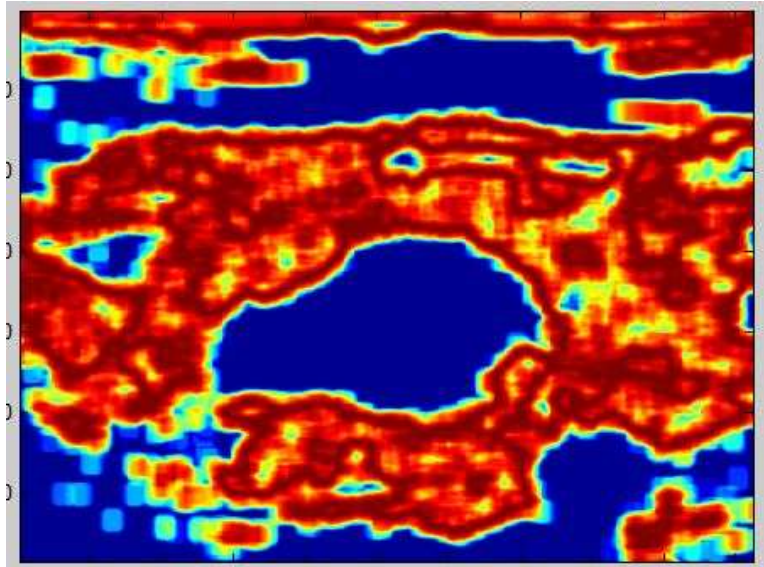


Figure 6.7: Segmented Image (Horizontal cut based Entropy Filtering)

Step 06:

Binary Image Formation



Figure 6.8: Binary Segmented Image

Step 07:

Deleting Boundary & Corner connected regions



Figure 6.9: Deleting Boundary & Corner connected regions

Step 08:

Ranking the left regions

It means that the larger area should stay and other small area compare to larger area will be eliminated.

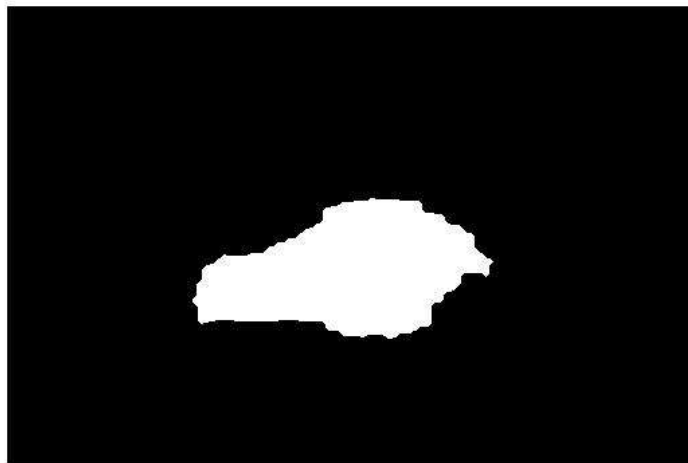


Figure 6.10: Ranking the binary image

Step 09:

Canny edge detection

The **Canny edge detector** is an edge detection operator that uses a multi-stage algorithm to detect a wide range of edges in images.

Edge detection, especially step edge detection has been widely applied in various computer vision systems, which is an important technique to extract useful structural information from different vision objects and dramatically reduce the amount of data to be processed. Canny has found that, the requirements for the application of edge detection on diverse vision systems are relatively the same. Thus, a development of an edge detection solution to address these requirements can be implemented in a wide range of situations.

The general criteria for edge detection includes

- Detection of edge with low error rate, which means that the detection should accurately catch as many edges shown in the image as possible
- The edge point detected from the operator should accurately localize on the center of the edge.
- A given edge in the image should only be marked once, and where possible, image noise should not create false edges.

The Process of Canny edge detection algorithm can be broken down to 5 different steps:

- Apply Gaussian filter to smooth the image in order to remove the noise
- Find the intensity gradients of the image
- Apply non-maximum suppression to get rid of spurious response to edge detection
- Apply double threshold to determine potential edges

- Track edge by hysteresis: Finalize the detection of edges by suppressing all the other edges that are weak and not connected to strong edges.

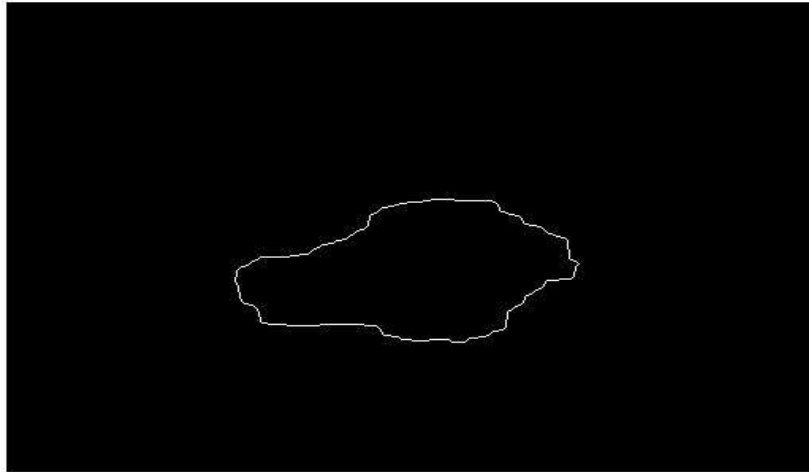


Figure 6.11: Applied canny edge detection

Step 10:

Superimpose detected edge output into main image

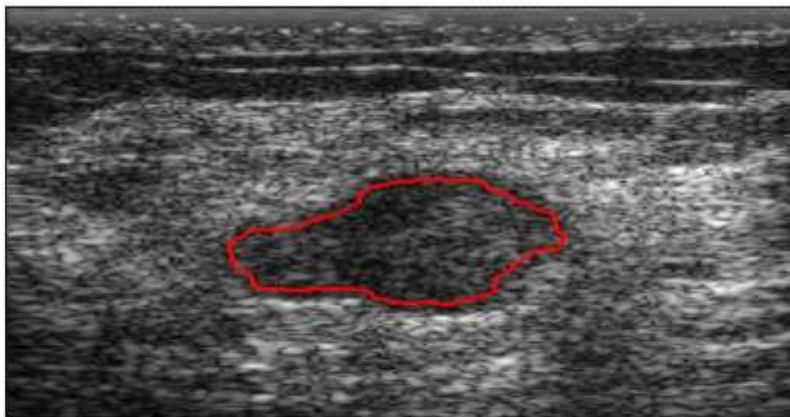


Figure 6.12: Edge detection image superimposed into BUS image

Results of different types of ultrasound image by applying region growing segmentation method:

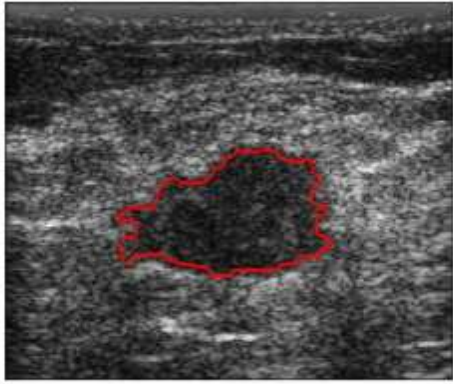


Figure 6.13: Our segmented image (Type-1)

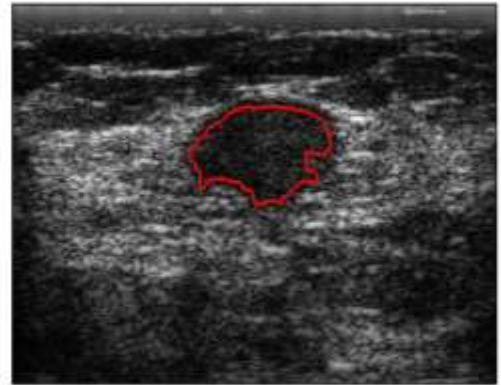


Figure 6.14: Our segmented image (Type-2)

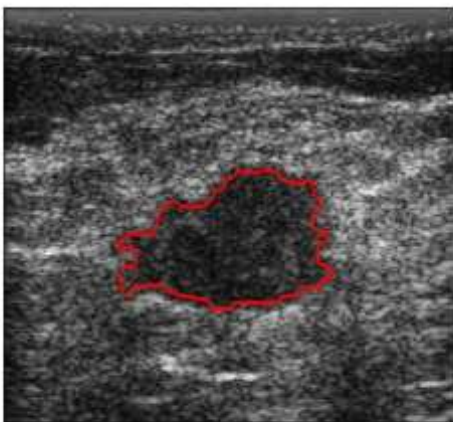


Figure 6.15: Our segmented image (Type-3)

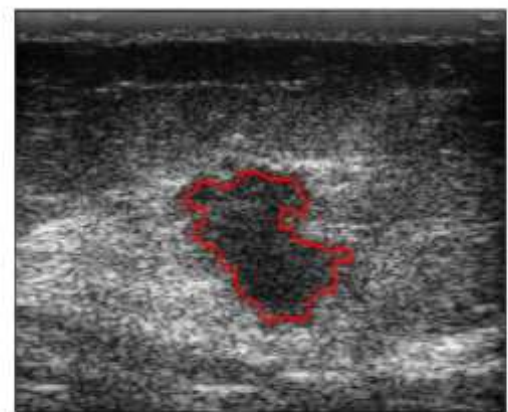


Figure 6.16: Our segmented image (Type-4)

# Chapter 07

## Conclusion

In this thesis, we came up a segmentation algorithm which is capable of detect lesion manually. Though our system successfully detect lesion but here human interaction needed because of manual seed selection.

### Problems of manual seed selection

- Manual method of segmentation is good but not effective for segmentation of large data sets.
- It is time consuming.
- Need of human interaction.

### Problems We faced

- Segmentation result is poor for the overshadowed ultrasound images.
- Edge detection is quite good for a particular data sets; not for all image data sets.
- Seed selection is manual.
- The result from Watershed method is not pretty good.

By researching over the different methods of segmentation we found out Region Growing Method more convenient and easier to detect the desired lesion. We approached by selecting the seed manually

Potential Future works may have listed as follows:

- Automatic seed selection
- Solving the problems in ROI detection phase
- Modelling of Shadowing Artifact of BUS image
- Improving Automatic Segmentation of detected ROI image

# Reference

- [1] Garcia, M., Jemal, A., Ward, E., Center, M., Hao, Y., Siegel, R., and Thun, M. Global Cancer Facts & Figures 2007, American Cancer Society, 2007.
- [2] American Cancer Society, Cancer Facts & Figures 2008, American Cancer Society, 2008.
- [3] American Cancer Society, Cancer Facts & Figures 2009, American Cancer Society, 2009.
- [4] American Cancer Society, Breast Cancer Facts & Figures 2007-2008, American Cancer Society, 2008.
- [5] World cancer research fund International  
<http://www.wcrf.org/int/cancer-facts-figures/worldwide-data>.
- [6] World cancer research fund International  
<http://www.wcrf.org/int/cancer-facts-figures/worldwide-data>.
- [7] World cancer research fund International  
<http://www.wcrf.org/int/cancer-facts-figures/worldwide-data>.
- [8] <http://www.cancer.org/cancer/breastcancer/detailedguide/breast-cancer-diagnosis>
- [8] Committee on Technologies for the Early Detection of Breast Cancer, Mammography and Beyond: Developing Technologies for the Early Detection of Breast Cancer, S.J. Nass, I.C. Henderson, and J.C. Lashof, Eds. National Cancer Policy Board, Institute of Medicine, and Commission on Life Studies, National Research Council, 2001.
- [9] Xu Liu, Zhimin Huo and Jiwu Zhang. Automated segmentation of breast lesions in ultrasound images. Proceedings of the 2005 IEEE Engineering in Medicine and Biology, 27th Annual Conference Shanghai, China, September 1-4, 2005
- [10] E. J. Bond, X. Li, S. C. Hagness, B.D. Van Veen, "Microwave Imaging via Space-Time Beamforming for Early Detection of Breast Cancer", IEEE Trans. Ant. Propag., vol. 51, no. 8, Aug. 2003.
- [11] X. Li and S.C. Hagness, "A confocal microwave imaging algorithm for breast cancer detection," IEEE Microwave Wireless Components Lett., vol. 11, pp. 130-32, Mar. 2001.
- [12] S.C. Hagness, A. Taflove, and J.E. Bridges, "Two-dimensional FDTD analysis of a pulsed microwave confocal system for breast cancer detection: fixed-focus and antenna array sensors", IEEE Trans. Biomed. Eng., vol. 45, pp. 1470-1479, Dec. 1998.

- [13] O. Husby and H. Rue, "Estimating blood vessel areas in ultrasound images using a deformable template model," *Statist. Model.*, vol. 4, no.3, pp. 211–226,2004.
- [35] A. Stavos, D. Thickman, C. Rapp, M. Dennis, S.Parker, and S. G. A., "Solid breast modules: Use of sonography to distinguish between benign and malignant lesions," *Radiology*, vol. 196, pp. 123–134, 1995.
- [36] V. Jackson, "Management of solid breast modules: What is the role of sonography?," *Radiology*, vol. 196, pp. 14–15, 1995.
- [37] P. Arger,C. Sehgal, E. Conant, J. Zuckerman, S. Rowling, and J. Patton, "Interreader variability and predictive value of is descriptions of solid masses: Pilot study," *Acad. Radiol.*, vol. 8, pp. 335–342,2001.
- [38] Cobbold, Richard S. C. (2007). *Foundations of Biomedical Ultrasound*. Oxford University Press. pp. 422–423
- [39] Merritt, CR (1 November 1989). "Ultrasound safety: what are the issues?". *Radiology* 173 (2): 304–306.
- [40] "Training in Diagnostic Ultrasound: essentials, principles and standards" (PDF). WHO. 1998. p. 2.
- [41] Stavros AT, Thickman D, Rapp CL et - al. Solid breast nodules: use of sonography to distinguish between benign and malign ant lesions. *Radiology*. 1995;196 (1): 123-34.
- [42] Rahbar G, Sie AC, Hansen GC et -al. Benign versus malignant solid breast masses: US differentiation. *Radiology*. 1999;213 (3): 889-94.
- [43] Cardeñosa G. *Clinical breast imaging, a patient focused teaching fi le*. Lippincott Williams & Wilkins. (2006)
- [44] Paredes ES. *Atlas of mammography*. Lippincott Williams & Wilkins. (2007)
- [45] Moi Hoon Yap, Eran A. Edirisinghe, and Helmut E. Bez, 2008, A novel algorithm for initial lesion detection in ultrasound breast images
- [47] K. Horsch, M. L. Giger, L. A. Venta, and C. J. Vyborny, "Automatic segmentation of breast lesions on ultrasound," *Med. Phys.*, vol. 28, no. 8, pp. 1652–1659, Aug. 2001.
- [48] ———, "Computerized diagnosis of breast lesions on ultrasound," *Med. Phys.*, vol. 29, no. 2, pp. 157–164, Feb. 2002.
- [49] K. Horsch, M. L. Giger, C. J. Vyborny, and L. A. Venta, "Perfor-mance of computer-aided diagnosis in the interpretation of lesions on breast sonography," *Acad. Radiol.*, vol. 11, no. 3, pp. 272–280, Mar. 2004. Bibliography
- [50] K. Drukker, M. L. Giger, K. Horsch, C. J. Kupinski, M. A. Vyborny, and E. B. Mendelson, "Computerized lesion detection on breast ultra-sound," *Med. Phys.*, vol. 29, no. 7, pp. 1438–1446, Jul. 2002.
- [51] D. R. Chen, R. F. Chang, W. J. Kuo, M. C. Chen, and Y. L. Huang, "Diagnosis of breast tumors with sonographic texture analysis using wavelet transform and neural networks," *Ultrasound Med. Biol.*, vol. 28, no. 10, pp. 1301–1310, Oct. 2002.



- [52] Y. L. Huang and D. R. Chen, "Watershed segmentation for breast tumor in 2-D sonography," *Ultrasound Med. Biol.*, vol. 30, no. 5, pp. 625–632, May 2004.
- [53] D. Boukerroui, A. Baskurt, J. A. Noble, and O. Basset, "Segmentation of ultrasound images—multiresolution 2-D and 3-D algorithm based on global and local statistics," *Pattern Recognit. Lett.*, vol. 24, no. 4–5, pp. 779–790, Feb. 2003.
- [54] G. F. Xiao, M. Brady, J. A. Noble, and Y. Y. Zhang, "Segmentation of ultrasound B-mode images with intensity inhomogeneity correction," *IEEE Trans. Med. Imag.*, vol. 21, no. 1, pp. 48–57, Jan. 2002.
- [55] Haralick, R. M., K. Shanmugam, and I. Dinstein, "Textural features for image classification," *IEEE Transactions on Systems, Man, and Cybernetics*, SMC-3, pp. 610–621, 1973.
- [56] Paredes ES. *Atlas of mammography*. Lippincott Williams & Wilkins. (2007)
- [57] Haralick, R.M., "Statistical and Structural Approaches to Texture," *Proceedings of the IEEE*, 67, pp. 786–804, 1979.
- [58] Zucker, S. W. and K. Kant, "Multiple -level Representations for Texture Discrimination," In *Proceedings of the IEEE Conference on Pattern Recognition and Image Processing*, pp. 609–614, Dallas, TX, 1981.
- [59] Breast Cancer Survival Rate  
<http://cancer753.blogspot.com/2013/05/breast-cancer-survival-rate.html>
- [60] The Watershed Transform: Strategies for Image Segmentation  
<http://www.mathworks.com/company/newsletters/articles/the-watershed-transform-strategies-for-image-segmentation.html>
- [61] Marker-Controlled Watershed Segmentation  
<http://www.mathworks.com/help/images/examples/marker-controlled-watershed-segmentation.html>
- [62] U.S. Food and Drug Administration  
<http://www.fda.gov/RadiationEmittingProducts/RadiationEmittingProductsandProcedures/MedicalImaging/ucm115357.htm>
- [63] How ultrasound imaging works explained simply  
[http://www.howequipmentworks.com/ultrasound\\_basics/](http://www.howequipmentworks.com/ultrasound_basics/)
- [64] Chan VWS. *Ultrasound Imaging for Regional Anesthesia*. 2nd ed. Toronto, ON: Toronto Printing Company; 2009.
- [65] Middleton W, Kurtz A, Hertzberg B. Practical physics. In: *Ultrasound, the Requisites*. 2nd ed. St Louis, MO: Mosby; 2004:3–27.
- [66] Hangiandreou N. AAPM/RSNA physics tutorial for residents: topics in US. B-mode US: basic concepts and new technology. *Radiographics*. 2003;23:1019–1033.
- [67] Liver B- Mode  
<http://www.medison.ru/uzi/eho478.htm>